Adaptivity Schemes for Model Predictive Speed Control of PMSM

Michal Kozubík
CEITEC - Central European Institute of Technology
Brno University of Technology
Brno, Czech Republic
Michal.Kozubik@ceitec.vutbr.cz

Pavel Václavek
CEITEC - Central European Institute of Technology
Brno University of Technology
Brno, Czech Republic
Pavel.Vaclavek@ceitec.vutbr.cz

Inigo Garcia de Madinabeitia Merino
AVL List GmbH
Graz, Austria
inigo.garciademadinabeitiamerino@avl.com

***Abstract*—Model predictive control is a popular research topic in the field of motor control. Its direct way of implementing constraints and nonlinearities makes MPC a potential alternative to standard motor control approaches. On the other hand, the control algorithm's dependency on the motor model's precision can make it tricky. Especially when the parameters of the controlled machine change over time. This paper presents a possible solution to a stated problem based on the model adaptivity. Firstly, the connection between experimental data and the parameters change is analyzed. Then, adaptivity schemes are presented. After that, the simulation experiment evaluates the performance of the proposed schemes.**

***Index Terms*—Predictive control, Nonlinear control, Adaptivity, Motor control, Permanent Magnet Synchronous Motor, Parameter mismatch**

I. Introduction

The industrial application of Permanent Magnet Synchronous Motors (PMSM) is becoming more prevalent thanks to the motor's high efficiency, precision, and overall performance. On the other hand, their nonlinear behavior can be challenging to handle by the control based on linear theory, such as PI control. Therefore, various modern complex methods of control are being applied to the problem, one of which is Model Predictive Control (MPC).

MPC offers a straightforward approach to problem definition and simple implementation of constraints and nonlinearities [1], [2]. On the other hand, it still poses an implementation challenge due to its computational demands, so the researchers focus on developing the methods that reduce them [3], [4]. The other challenge of MPC is its dependency on the model of the controlled plant.

The predictive controller uses measured data and a model of the controlled plant to compute the future values of states. The first thing that can affect the control algorithm's performance is the measurement disturbances. Standard methods, such as observers [5], [6], can solve the problem of measurement errors.

Even though the model of motor is usually considered time-invariant, all parameters do not remain the same, and these differences lead to the prediction errors [7]. Due to this parameter mismatch affecting the controller's output, the methods to increase the robustness are being developed [8]–[10].

Apart from robustness, the other common approach to mitigate the effect of parameter mismatch is adaptivity. [11], [12] The principle of adaptive control is to link the change of plant parameters to the change of designed control law. In this paper, we draw on this principle. Chosen approach only affects the model of the controlled plant and not the cost function, which is another essential part of MPC.

This paper analyzes the changes in motor parameters, which are linked to motor states. We present the adaptivity functions based on experimental data. The paper introduces two adaptivity schemes that update the model used in the prediction stage in every control step to solve the parameter mismatches. Experiments compare presented schemes with the controller without any update.

The paper's organization is as follows: In Section II, we present our control problem. First, we present the general mathematical model of PMSM in the *dq*-reference frame. The description of the predictive controller follows, including the common principle of predictive control. The final part of Section I describes the change of parameters based on experimental data. Section III proposes and describes two adaptivity schemes, each focusing on different drawbacks of adaptivity in our designed control. In Section IV, the experiment in Matlab Simulink is performed, and the results are presented. The experiment focused on the ability of each other controller to track the requested value of angular speed. Secondly, the experiment tested the ability of the controller to keep the requested states within their limits.

Section V summarizes the paper and explains the achieved results. Furthermore, it describes the outcomes of the presented adaptivity schemes.

II. Preliminaries

A. Plant

For the description of plant, we use the generic model of PMSM in *dq*-reference frame

$$\begin{aligned}\frac{\mathrm{d}i_d}{\mathrm{d}t} &= -\frac{R_s}{L_d}i_d + P_p\frac{L_q}{L_d}i_q\omega_m + \frac{1}{L_d}u_d\\ \frac{\mathrm{d}i_q}{\mathrm{d}t} &= -\frac{R_s}{L_q}i_q - P_p\frac{L_d}{L_q}i_d\omega_m - \frac{Pp\Psi_{PM}}{L_q}\omega_m + \frac{1}{L_q}u_q \\ \frac{\mathrm{d}\omega_m}{\mathrm{d}t} &= \frac{3}{2}\frac{P_p}{J}\left(\Psi_{PM}i_q + (L_d - L_q)\, i_d i_q - T_l\right),\end{aligned} \tag{1}$$

where

i_d, i_q	are stator current components in *dq*-frame,
u_d, u_q	are stator voltage components in *dq*-frame,
ω_m	is rotor mechanical angular speed,
T_l	is load torque,
P_p	is number of pole pairs,
R_s	is stator winding resistance,
L_d, L_q	are rotor inductance components,
Ψ_{PM}	is permanent magnet flux,
J	is the moment of inertia.

B. Controller

We designed the predictive controller to control the speed of PMSM. The idea of Model Predictive Control is to use the model of controlled plant and measured states to predict and optimize future system behavior. The trajectory of states is computed across a pre-defined prediction horizon. Next, the algorithm computes the optimal control for this prediction horizon. Finally, the control for the first prediction step is applied to the plant. [13], [14]

For the presented adaptivity schemes we presume the typical structure of the control algorithm consisitng of *Prediction* step in which we use the model of the controlled plant to compute the future values of the plant's states. The second necessary step *Cost Function Evaluation* assigns the value of the cost function to a generated solution. The other steps specific to the used optimization algorithm follow.

We apply the presented schemes to the predictive controller working on the continuous control set. We consider the incremental form of controller

$$\mathbf{u}_{d,q|k+1} = \begin{bmatrix} u_{d|k+1} \\ u_{q|k+1}\end{bmatrix} = \begin{bmatrix} u_{d|k} \\ u_{q|k}\end{bmatrix} + \begin{bmatrix} \Delta u_{d|k} \\ \Delta u_{q|k}\end{bmatrix} \tag{2}$$

thus the control set is the set of voltage increment vectors. In the experiments, the parameters of the model used in the *Prediction* step will change according to chosen adaptivity scheme and obtained adaptivity functions. Both are described later in the paper.

C. Analysis of parameter change

To suppress the effect of the temperature, the measurements were performed while the constant temperature was held.

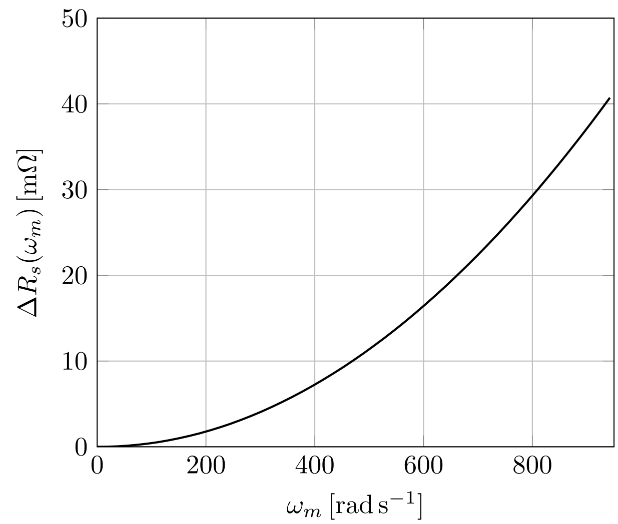

Fig. 1. Change of the stator resistance based on the speed of rotor.

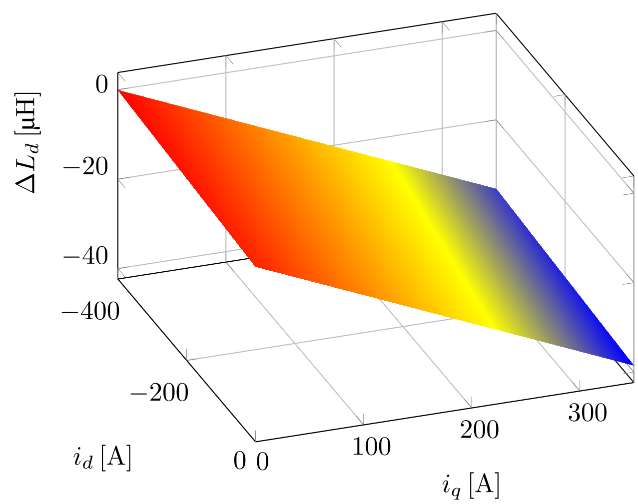

Fig. 2. Change of the direct part of inductance based on the current.

1) Resistance change: Measurements have shown the connection between the rotor speed and the increase of stator resistance. Figure 1 shows the dependency of the change of stator resistance on the speed of the rotor. Based on this information, we can state the equation used to evaluate the stator resistance.

$$R_s = R_{s0} + \Delta R_s(\omega_m). \tag{3}$$

2) Inductance change: We found the connection between the change of inductances and stator current. As the current consists of two parts, the function of change is more complex than the function of the stator resistance. Figures 2 and 3 show the 3d plot of the dependency of the change of direct and quadrature part of inductance on the compounds of stator current.

Similarly to the equation (3), the change of inductances can

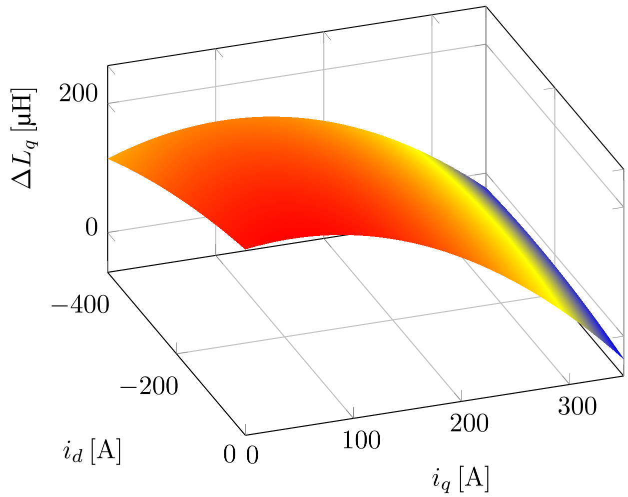

Fig. 3. Change of the quadarture part of inductance based on the current.

be described by the functions

$$L_d = L_{d0} + \Delta L_d(i_d, i_q) \tag{4}$$
$$L_q = L_{q0} + \Delta L_d(i_d, i_q). \tag{5}$$

Inverse values of inductances are present in the model 1. Therefore, it is convenient to compute them beforehand for better performance of the control algorithm.

III. Proposed adaptivity schemes

In this paper, we propose two adaptivity schemes, each representing some trade-off between precision and execution speed. The second mentioned is essential in the case of motor control due to the short sampling times necessary for the correct performance. Figures showing the presenting schemes consist of blocks that represent pre-defined functions:
Measurement represents obtaining the values of states $\mathbf{x}$, their filtration, and manipulation, e.g., Clarke and Park transformation.
Adaptivity Algorithm is responsible for calculating the parameters $\mathbf{P}$ of the model. This block can contain any parameter estimation method, e.g., [15]–[17]. For the demonstration purpose, this block evaluates the functions of parameter change obtained and described before.
Predictive Controller block computes the optimal control value. The algorithm uses measured states $\mathbf{x}$ and calculated parameters $\mathbf{P}$ for the prediction.
Control Value Application block ensures the correct transfer of control value to plant, e.g., inverse transformations.

A. In-line scheme

The first scheme is the In-line scheme. Figure 4 shows the structure of the scheme. The measured data are used immediately for the adaptivity algorithm, therefore the parameters $\mathbf{P}$ used for the prediction are given by the adaptivity function $f_a()$ and measured states $\mathbf{x}_k$

$$\mathbf{P}_k = f_a(\mathbf{x}_k). \tag{6}$$

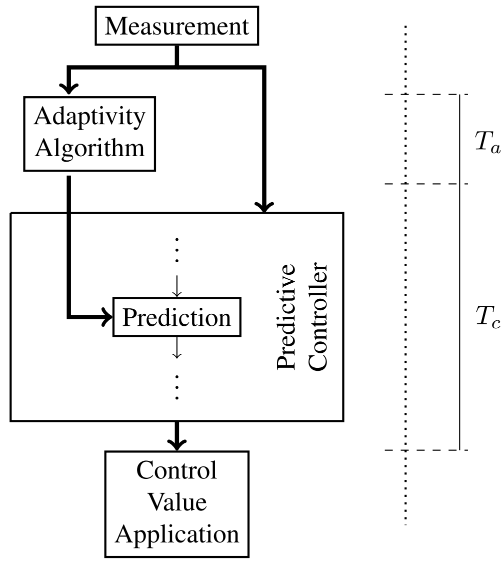

Fig. 4. In-line scheme

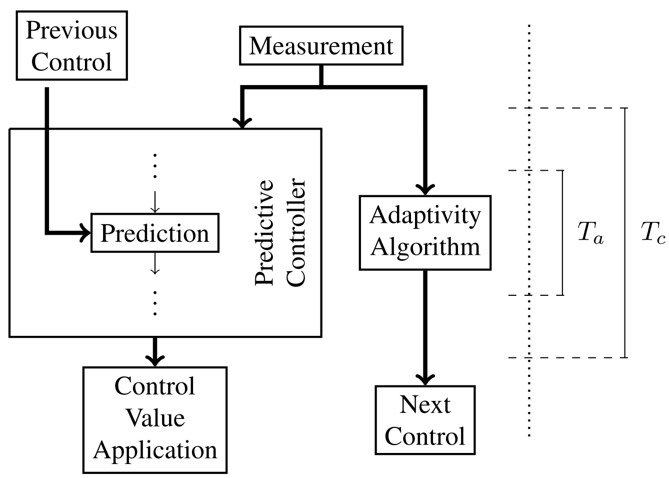

Fig. 5. Parallel scheme

As the Adaptivity Algorithm block is executed before the predictive control, the time requested by the Adaptivity Algorithm T_a prolongs the time necessary to compute the control value T_c.

B. Parallel scheme

Figure 5 shows the structure of the second presented scheme. As the scheme suggests, the algorithm is executed parallelly to the control algorithm. The parameters $\mathbf{P}$ used for the prediction are given by the adaptivity function $f_a()$ and states measured in the previous control step

$$\mathbf{P}_k = f_a(\mathbf{x}_{k-1}). \tag{7}$$

This delay can affect the precision of the prediction. On the other hand, assuming $T_a < T_c$, the adaptivity algorithm does not affect the execution time.

TABLE I
PARAMETERS OF PMSM

Parameter	Value	
R_{s0}	22.84	mΩ
L_{d0}	0.48	mH
L_{q0}	0.78	mH
Ψ_{PM}	163.8	mWb
Pp	4	
J	11.25×10^{-3}	$\mathrm{kg\,m^2}$
U_{DC}	500	V
I_R	310	A

TABLE II
PARAMETERS OF THE CONTROLLER

Parameter	Value
w_{ST}	1
w_{i_d}	0.001
w_{i_d}	0.005
w_I	100
w_U	100
N	4
T_s	100 µs

IV. SIMULATION RESULTS

We tested the presented schemes in PIL co-simulation consisting of a control algorithm implemented on Jetson Xavier and the model of PMSM in Simscape. Table 1 shows the parameters of PMSM.

For the control, we used the algorithm presented in [18]. The Table II shows the parameters of the control algorithm and the table III shows the Differential Evolution algorithm parameters used to solve the optimization problem.

We measured the time necessary to execute control and adaptivity algorithms properly. The average execution time of control algorithm T_c was $50\,\mu s$. The time required by the adaptivity algorithm T_a was on average $15\,\mu s$. Thus, as mentioned before, the adaptivity algorithm did not affect the time necessary to calculate the control value properly.

The reference signal consisted of the initial ramp raising to the value of $900\,\mathrm{rad\,s^{-1}}$. Then, the constant value followed until the angular speed of the rotor settled. Next, the decreasing ramp followed, which tested, whether the ability of the controller to ensure the tracking of such type of request changed or not. Finally, a constant value of zero was requested. We performed the experiment without any load torque.

A. Angular speed

Figure 6 shows the results achieved by different approaches. The controller without any adaptivity algorithm could not reach the requested value of angular speed. The difference between the requested value and the result was $1\,\%$ of the requested value. The controller ensured the tracking of the ramp and the zero signals, similar to the other tested approaches.

Both controllers with presented adaptivity schemes were able to reach the requested value of $900\,\mathrm{rad\,s^{-1}}$, track

TABLE III
PARAMETERS OF DIFFERENTIAL EVOLUTION

Parameter	Value
Number of Agents	512
Number of Generations	20
t_r	0.5
s	0.6

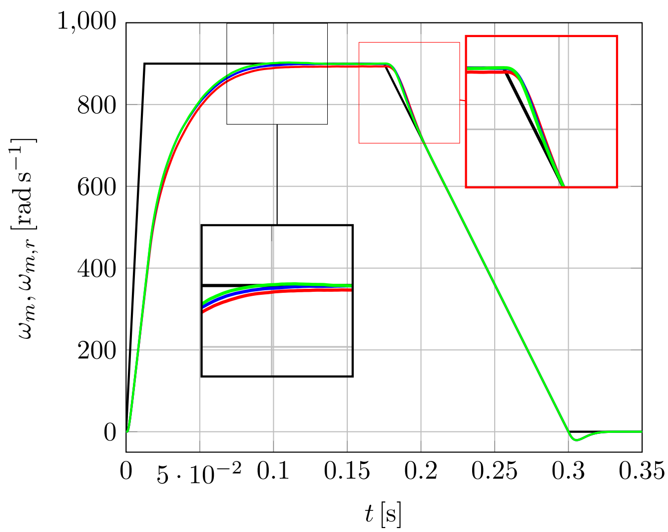

Fig. 6. Results of the experiment; black - reference, red - no adaptivity scheme, blue - parallel adaptivity scheme, green - in-line adaptivity scheme.

the ramp signal and zero signal. As the figure shows, the controller with an in-line scheme performed slightly faster.

B. Torque

An essential factor of the speed control is torque generated by the motor. Figure 7 shows the torque generated by the motor for each approach. Here, the slight change of motor dynamics caused by the change of parameters led to lower maximal torque generated by the motor controlled by the controller without adaptivity. Lower generated torque led to a slower rise of angular speed and caused the difference between the requested value and the result. Similarly, when was the motor slowing down, there was an apparent difference in generated torque for the distinctive approach, but the consequences of this difference were not so significant.

C. Current

The current has a direct link to the generated torque. The crucial part about current in the motor control is to keep it within pre-defined limits. Even though some overshoot of rated current I_R is usually allowed for a short time, we try not to overstep this value in our implementation. Figure 8 shows the currents in *dq*-frame and the limit I_R. The observed current did not overshoot the defined limit for any tested approach. The maximal current for all approaches reached $98\,\%$ of I_R. The figure also shows similar behavior for both adaptivity schemes. The difference occurred again in the case without any adaptivity. As the figure shows, the controller tended to

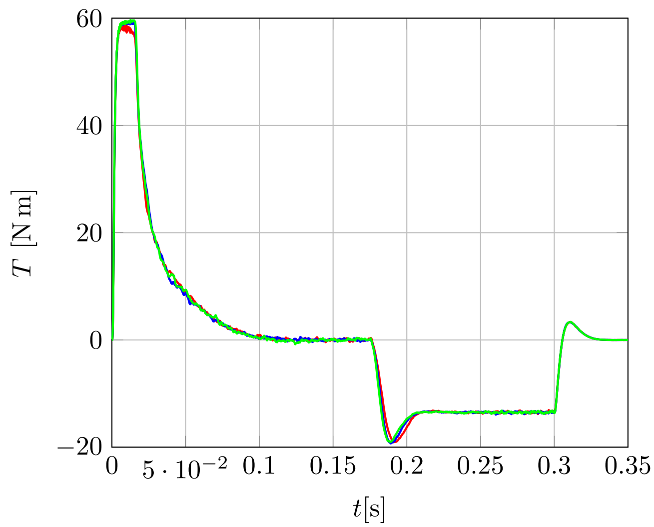

Fig. 7. Torque during experiment; red - no adaptivity scheme, blue - parallel adaptivity scheme, green - in-line adaptivity scheme.

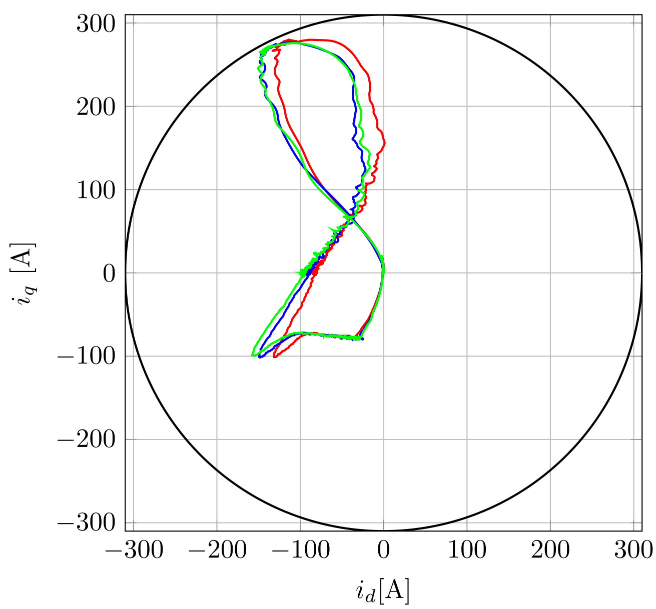

Fig. 8. Currents in dq reference frame; red - no adaptivity scheme, blue - parallel adaptivity scheme, green - in-line adaptivity scheme.

favor the quadrature part of the current. Missing information about the change of inductances, which affects the reluctance component of torque, caused this. Different values of current led to differences in the generated torque described before.

D. Voltage

Finally, the voltage acts as an input in the model (1). As such, it underlies constraints given by the voltage of a supply V_{DC}. Figure 9 shows the voltages in dq-frame and mentioned constraint. All calculated voltages satisfied the constraint. The controllers performed similarly with the difference, which appeared again in the case of control without adaptivity. This

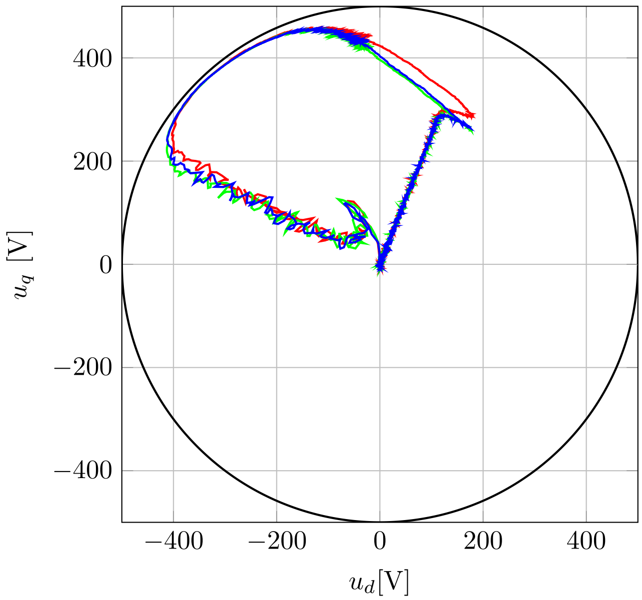

Fig. 9. Voltages in dq-reference frame; red - no adaptivity scheme, blue - parallel adaptivity scheme, green - in-line adaptivity scheme.

difference led to the behavior described before. Because we consider the voltage as the controller's output, its value is directly connected to the precision of the model and thus is affected by the differences.

V. Conclusion

Experimental data has shown that parameters of PMSM, such as resistance and inductances, are not time-invariant. This paper analyzed the changes and presented a possible approach to mitigating such changes. Two adaptivity schemes were presented. First of them, focusing on the model's precision but prolonging the control algorithm's execution time. The second one does not affect the execution time. On the other hand, the adaptivity function does not work with actual data.

Presented schemes were compared in PIL co-simulation with the control algorithm implemented in GPU and Simscape model of the motor. The experiment also contained the control without any adaptivity scheme for comparison.

The results have shown that the change in plant parameters affects the control algorithm's overall performance, e.g., the controller without any adaptivity scheme could not reach the requested value of angular speed. On the other hand, there was no significant difference between the controller's performance with the In-line adaptivity scheme or the Parallel one. These results favor the second-mentioned because its execution does not affect the computation time, which is crucial in motor control.

The results open new possibilities for experiments, e.g., testing presented schemes on a real physical system affected by outer agents will lead to a need to use more sophisticated identification methods.

VI. Acknowledgement

The completion of this paper was made possible by the grant No. FEKT-S-20-6205 - "Research in Automation, Cybernetics and Artificial Intelligence within Industry 4.0" financially supported by the Internal science fund of Brno University of Technology.

The work has been performed in the project NewControl: Integrated, Fail-Operational, Cognitive Perception, Planning and Control Systems for Highly Automated Vehicles, under grant agreement No 826653/8A19006. The work was co-funded by grants of Ministry of Education, Youth and Sports of the Czech Republic and Electronic Component Systems for European Leadership Joint Undertaking (ECSEL JU).

The work was supported by the infrastructure of RICAIP that has received funding from the European Union's Horizon 2020 research and innovation programme under grant agreement No 857306 and from Ministry of Education, Youth and Sports under OP RDE grant agreement No CZ.02.1.01/0.0/0.0/17_043/0010085.

References

[1] T. Tarczewski and L. M. Grzesiak, "Constrained state feedback speed control of pmsm based on model predictive approach," *IEEE Transactions on Industrial Electronics*, vol. 63, no. 6, pp. 3867–3875, 2015.

[2] F. Wang, S. Li, X. Mei, W. Xie, J. Rodriguez, and R. M. Kennel, "Model-based predictive direct control strategies for electrical drives: An experimental evaluation of ptc and pcc methods," *IEEE Transactions on Industrial Informatics*, vol. 11, no. 3, pp. 671–681, 2015.

[3] T. Geyer and D. E. Quevedo, "Performance of multistep finite control set model predictive control for power electronics," *IEEE Transactions on Power Electronics*, vol. 30, no. 3, pp. 1633–1644, 2015.

[4] M. Siami, D. A. Khaburi, M. Rivera, and J. Rodriguez, "A computationally efficient lookup table based fcs-mpc for pmsm drives fed by matrix converters," *IEEE Transactions on Industrial Electronics*, vol. 64, no. 10, pp. 7645–7654, 2017.

[5] B. Wang, X. Chen, Y. Yu, G. Wang, and D. Xu, "Robust predictive current control with online disturbance estimation for induction machine drives," *IEEE Transactions on Power Electronics*, vol. 32, no. 6, pp. 4663–4674, 2016.

[6] S. Huang, G. Wu, F. Rong, C. Zhang, S. Huang, and Q. Wu, "Novel predictive stator flux control techniques for pmsm drives," *IEEE Transactions on Power Electronics*, vol. 34, no. 9, pp. 8916–8929, 2019.

[7] H. A. Young, M. A. Perez, and J. Rodriguez, "Analysis of finite-control-set model predictive current control with model parameter mismatch in a three-phase inverter," *IEEE Transactions on Industrial Electronics*, vol. 63, no. 5, pp. 3100–3107, 2016.

[8] M. S. R. Saeed, W. Song, and B. Yu, "Robustness improvement of deadbeat model predictive control for five-phase pmsm drives," in *2020 15th IEEE Conference on Industrial Electronics and Applications (ICIEA)*, pp. 1336–1341, 2020.

[9] X. Yuan, S. Zhang, and C. Zhang, "Enhanced robust deadbeat predictive current control for pmsm drives," *IEEE Access*, vol. 7, pp. 148218–148230, 2019.

[10] Z. Li, F. Wang, D. Ke, J. Li, and W. Zhang, "Robust continuous model predictive speed and current control for pmsm with adaptive integral sliding-mode approach," *IEEE Transactions on Power Electronics*, vol. 36, no. 12, pp. 14398–14408, 2021.

[11] S.-Y. Kim, W. Lee, M.-S. Rho, and S.-Y. Park, "Effective dead-time compensation using a simple vectorial disturbance estimator in pmsm drives," *IEEE Transactions on Industrial Electronics*, vol. 57, no. 5, pp. 1609–1614, 2010.

[12] S. Li and Z. Liu, "Adaptive speed control for permanent-magnet synchronous motor system with variations of load inertia," *IEEE transactions on industrial electronics*, vol. 56, no. 8, pp. 3050–3059, 2009.

[13] L. Grüne and J. Pannek, *Nonlinear model predictive control*. Springer, 2017.

[14] E. F. Camacho and C. B. Alba, *Model predictive control*. Springer science & business media, 2013.

[15] Y. Yu, X. Huang, Z. Li, M. Wu, T. Shi, Y. Cao, G. Yang, and F. Niu, "Full parameter estimation for permanent magnet synchronous motors," *IEEE Transactions on Industrial Electronics*, vol. 69, no. 5, pp. 4376–4386, 2022.

[16] P. Sun, Q. Ge, B. Zhang, and X. Wang, "Sensorless control technique of pmsm based on rls on-line parameter identification," in *2018 21st international conference on electrical machines and systems (ICEMS)*, pp. 1670–1673, IEEE, 2018.

[17] X. Li and R. Kennel, "General formulation of kalman-filter-based online parameter identification methods for vsi-fed pmsm," *IEEE Transactions on Industrial Electronics*, vol. 68, no. 4, pp. 2856–2864, 2020.

[18] M. Kozubik and D. Friml, "Differential evolution based nonlinear model predictive speed control of pmsm implemented on gpu," in *2021 IEEE 30th International Symposium on Industrial Electronics (ISIE)*, pp. 1–6, IEEE, 2021.